International Congress of Science and Technology of Metallurgy and Materials, SAM – CONAMET 2014

Raman scattering applied to materials science

Andrés Cantarero

Materials Science Institute, University of Valencia, PO Box 22085, 46071 Valencia, Spain

Abstract

One of the most powerful techniques to extract physical and chemical information of a material is the light scattering. Opposite to x-ray scattering for instance, where an average of the sample properties is obtained, Raman scattering is a local probe which can be used to detect inhomogeneities, local strain, lack of crystallinity, anharmonicities or information on the electronic structure by means of resonant Raman scattering. In this work, we will analyze the main contributions of Raman scattering in Materials Sciences. After a brief introduction of the technique and the equipment needed for the physical measurements, we will give practical examples of Raman scattering measurements applied to a number of materials and the valuable information obtained in every example.
Keywords: Raman scattering; materials science; semiconductors; insulators

1. Introduction

Raman scattering or light scattering consists of the absorption of a photon, the emission or absorption of a phonon, and finally the emission of a photon. In the case of phonon emission the process is called Stokes, while in the case of phonon absorption it is called anti-Stokes. In a Stokes process the energy of the emitted photon is smaller than that of the absorbed photon, while in the case of anti-Stokes, it is larger. In the last case, phonons must be present in the material, what means that the temperature must be high (the Bose-Einstein factor should not be negligible compare to one). At very low temperatures, only the Stokes processes are observed. The difference between the laser source wave number and that of the emitted phonon is called Raman shift (Stokes or anti-Stokes), i.e. we have an identical energy spectrum at the left and right sides of the laser (only the intensity is different). In the description given above we have described the so called spontaneous Raman scattering. The population of the emitted phonons in a Stokes process is proportional to $N_0 + 1$, where N_0 is the phonon population (in practice the Bose-Einstein distribution function). In the anti-Stokes process the signal is proportional to N_0, thus at low temperature where the phonon population is low

---

∗ Corresponding author. Tel.: +34-963-54-44713 ; fax: +34-963-54-3633.
   E-mail address: cantarer@uv.es

it cannot be observed. There is a technique, called CARS [Cantarero (2012)], where phonons are excited at the anti-Stokes frequency and the signal can be several orders of magnitude larger. In that case, we are dealing with stimulated Raman scattering. Unfortunately, although the technique is very powerful we need two laser sources with a difference in wave numbers equal to the phonon wave number.

When the Raman signal is too weak to be observed, as it can be the case of a tiny amount of material or a few molecules (or a cell), there is a technique called SERS which consists of attach to the material a gold or silver sphere or star [Hamon et al. (2014)] in order to couple the plasmon of the silver or the gold with the phonon. In that case, it has been shown that the Raman signal can be improve 6-8 orders of magnitude. A similar technique, with the same physics, is that using the tip of a AFM to enhance the signal. The tip is metallized. The technique, called TERS, is becoming more popular in the study of tiny amounts of materials on top of a surface. Since the technique is based on SNOM, a xy scanning is necessary [Cantarero (2012)].

The Raman spectrum or Raman shift is characteristic from a material, thus Raman scattering can be used to identify the material. On the other hand, it is an optical technique, i.e. we do not need to destroy the material as in the case of other analysis techniques like XRD.

By means of Raman scattering it is possible to analyze the micro-crystallinity by using the polarization properties, or the polarization with polar diagrams [Möller et al.(2011)], to measure the stress of the sample from the phonon shift (PDP) [Anastassakis et al.(1990)], to measure the electron concentration from the splitting of the polar phonons [Segura-Ruiz et al. (2008)], to obtain the Grüneisen parameters [Camacho et al. (2002), Ulrich et al. (1996)] the variation of the gap with temperature [Olguin et al. (2002)], study of defects [Villafuerte et al. (2014)], anharmonicity [Anastassakis et al. (1990)], phonon confinement [Comas et al. (1995)], Raman shift due to isotopic content [Widulle et al. (1999)] and many other material properties.

Nomenclature

RRS	Resonant Raman scattering
CARS	Coherent anti-Stokes Raman scattering
SERS	Surface enhanced Raman spectroscopy
AFM	Atomic force microscopy
TERS	Tip enhanced Raman scattering
SNOM	Scanning near field optical microscopy (also NSOM)
XRD	X-ray diffraction
PL	Photoluminescence
PM	Photomultiplier
CCD	Charge coupled device
PDP	Phonon deformation potentials
TO	transversal optical
LO	longitudinal optical
PSA	Prostate specific antigen
HOPG	Highly ordered pyrolytic graphite

---

2. The Raman effect

In 1922, León Brillouin [Brillouin (1922)] predicted the light scattering by sound waves of long wavelength. In the following year, Adolf Smekal [Smekal (923)] developed the theory of light scattering by two discrete levels. Finally, in 1928, Chandrasekhara Ventaka Raman [Raman (1928)] discovered the light scattering at finite wavelengths. Raman used the Sun as light source, a telescope as a collector and the eye as a detector. The same year, Grigory Landsberg and Leonid Maldelstam discovered the same effect [Landsberg and Mandelstam (1928)]. This last article was published in July 13th, while the article of Raman was published previously. C. V. Raman got the Nobel Prize for the discovery of this effect in 1930. The difference between Raman and Brillouin scattering is semantic, it is basically the same
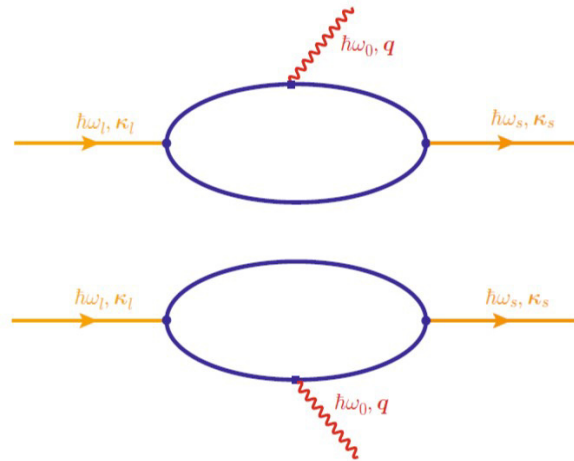
Fig. 1. Feynman diagrams of a Raman process.

effect. The scattering of phonons by light, either acoustic (Brillouin) or optical (Raman). But the equipment needed is different since in the case of Brillouin scattering we have to approach a few MHz to the laser light.

The Raman effect became very popular after the discovery of the laser as light source in the 60s of last century. The experiments have been done in the past with a double or triple spectrometer, to separate the Raman signal from the laser light, the laser as light source and a PM. Nowadays, a CCD is more commonly used as detector and a single spectrometer with a Notch or Edge filter to disperse the signal. If we do not need high resolution, a Raman systems can be very compact (actually portable). The PM however must be used when we need to perform high resolution experiments, the CCDs are limited by the pixel size, while the PM by the slit aperture.

The first distinction we have to do is to clarify the difference between a Raman and a IR experiment. In a IR experiment, the wavelength of the light is of the order of the wavelength of the phonons (optical) and there is a direct coupling between the electric field of the light (transverse to the propagation direction) and the TO phonons. Actually, there is a gap between the TO and the LO phonon and the people call them as IR bands [Cantarero (2013)]. The units in a IR spectrum are absolute units, while in Raman are relative to the laser frequency. In the case of a Raman experiment, the light has an energy closer to the electronic transitions, far from the direct phonon absorption and, as demonstrated by R. Loudon [Loudon (1963)], the electronic states are virtual intermediate states in the process. Since the Raman signal is referred to the laser light, this is the reason why it is called Raman shift. The energy of the light is in the range of the visible while the phonon energies are a few tenths of eV.

Also, it is important to distinguish between Raman and PL. In a PL experiment, the incoming photon has several times the energy of an optical phonon. Actually, the excited electron (or hole) thermalizes emitting optical and acoustic phonons until the only option is the radiative recombination. Raman scattering is a coherent process: one photon creates an electron-hole pair, either the electron or the hole emits a phonon (or absorbs a phonon) and finally the electron or hole recombines and produce a photon. The electronic system returns to its ground state, but there is one more phonon on it. The processes are described through the Feynman diagram given in Fig. 1.

2.1. Raman scattering efficiency

In a solid, the light penetrates a certain amount from the surface, depending on the wavelength and the properties of the material. In that case, it makes no sense to work with the scattering cross section since not all the volume is emitting a Raman signal. Instead, we define the scattering efficiency as the scattering cross section per unit volume [Cantarero et al. (1989)]:

$$\frac{dS}{d\Omega} = \frac{\omega_l \omega_s^3}{c^4} \frac{\hbar}{2V_c M^\star \omega_0} \frac{n_s}{n_l} (N_0 + 1) \sum_i \left| \vec{e}_s \mathcal{R}_i \vec{e}_l \right|^2 \tag{1}$$

where ω_l (ω_s) is the laser (scattered) frequency, V_c the volume of the unit cell, ω_0 the phonon energy, n_l (n_s) the refractive index of the laser (scattered) light, c the speed of light in vacuum, $M^{\star}$ the mass of the unit cell, $\vec{e}_l$ ($\vec{e}_s$) the polarization vector of the laser (scattered) light and $\mathcal{R}_i$ the Raman tensor component. In the case of ZB materials, the Raman tensor components are

$$\mathcal{R}_1 = \begin{pmatrix} 0\ 0\ 0 \\ 0\ 0\ d \\ 0\ d\ 0 \end{pmatrix} \quad ; \quad \mathcal{R}_2 = \begin{pmatrix} 0\ 0\ d \\ 0\ 0\ d \\ d\ 0\ 0 \end{pmatrix} \quad ; \quad \mathcal{R}_3 = \begin{pmatrix} 0\ d\ 0 \\ 0\ 0\ 0 \\ d\ 0\ 0 \end{pmatrix} \tag{2}$$

d being the Raman polarizability, written as

$$d = \frac{n_l n_s}{2\pi} \frac{V_c}{\bar{u}_0} \frac{1}{\hbar\omega_l} W_{fi}(\omega_l, \vec{e}_l, \omega_s, \vec{e}_s) \tag{3}$$

where $\bar{u}_0$ is the relative phonon displacement and the probability of a phonon emission is

$$W_{fi}(\omega_l, \vec{e}_l, \omega_s, \vec{e}_s) = \sum_{p,q} \frac{\langle f|\mathcal{H}_R|\rangle p \langle p|\mathcal{H}_L|q\rangle \langle q|\mathcal{H}_R|i\rangle}{(\hbar\omega_l - E_p + i\gamma_p)(\hbar\omega_s - E_q + i\gamma_q)} \tag{4}$$

where E_p and E_q are two intermediate electronic states in the process and γ_p and γ_q their corresponding broadening of the electronic states. When the laser energy or that of the scattered photon is of the order of the gap we call the process resonant Raman scattering. If the broadening of the electronic states is neglected (infinite lifetime), the probability tends to infinity. In that case we named the phenomenon as resonant Raman scattering. As a general fact, at low temperatures where the broadenings are lowers, the enhancement is larger.

3. Raman effect applied to Materials Science

We are going to give some examples of the Raman technique applied to the analysis of different properties of materials. We start with Ge quantum wires, where due to the very weak signal and the indirect band gap in the infrared (it is not possible to tune a laser around the gap), it is necessary to use TERS to have an observable signal. Due to limitation of space, it is not possible to explain in extend all possibilities openened with Raman scattering as a powerful non invasive technique. It can be applied not only to inorganic materials, but to organic or liquids (solutions). Every material has a characteristic Raman spectrum.

3.1. SERS and TERS

SERS consists of the coupling of the phonon with the plasmon of a gold (or silver) nanoparticle, not necessarily spherical [Hamon et al. (2014)]. Actually, in the case of stars, the electric field at the star tips enhances the signal much more than that of spherical nanoparticles. The technique is commonly used in biology, the metals being attached to proteins, cells, or cancer markers like PSA. It can be used also with inorganic molecules to enhance the Raman signal. For this purpuse, a special patterned substrate is needed to enhance properly the signal. In Materials Science however, it is becoming popular the use of TERS, i.e. instead of a gold nanoparticle, the tip of an AFM is used. An example is given in Fig. 2, where the enhancement of the Raman signal with the tip of a AFM can be observed in the case of a Ge nanowire [Ogawa et al. (2011)]. Although there are different configurations in TERS, the most commonly used is that where the incoming beam hit the sample from outside the microscope and the signal is collected in the region where the tip is within the laser spot region. Unfortunately, in both cases, since the resolution of the technique is given by the size of the tip (around 100 nm or even smaller) it is necessary a mapping around the sample in order to analyze it. This, on the other hand, increases the acquisition time.

3.2. Strain effects. Phonon deformation potentials

PDP are the coefficients giving the phonon shift due to the application of strain. The strain can be internal (for instance in the case of Ge-Si heterostructures) or external, due to the ensambling of electronic circuits for instance. The way to know the strain is to calibrate the phonon shift with pressure. In Fig. 3 (left panel) [Anastassakis el al.
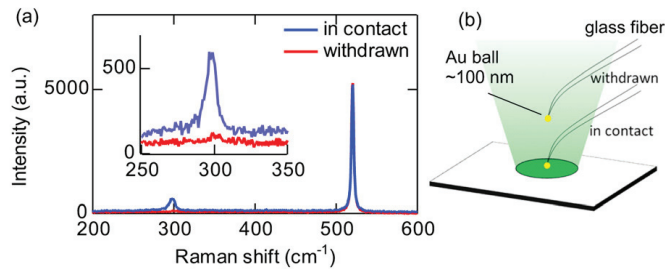
Fig. 2. (a) Raman spectra of a single Ge nanowire on a SiO2/Si substrate with the AFM tip in contact (blue line) and with the tip withdrawn (red line). (b) Experimental setup.
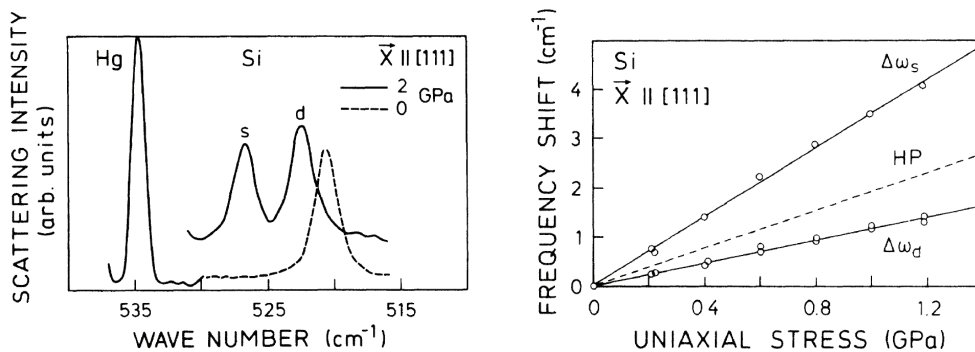

Fig. 3. Left panel: Singlet and doublet Raman peaks of silicon when an uniaxial stress is applied along the [111] direction. A line of a mercury lamp is used for calibration. Right panel: Phonon shift of Si with uniaxial stress. The dashed line corresponds to the shift due to hydrostatic pressure.

(1989)] they showed the phonon displacement when a Si bar was pressed along the [111] direction. In the figure at the left we can observe how the Si phonon at ambient pressure splits into two peaks, a singlet, along the stress direction, and a doublet, perpendicular to it. The peak of a Hg lamp was used for calibration purposes. From the measurements of bars cut along the [100], [110] and [111] directions, the PDPs can be obtained. In Fig. 3 (right panel) we can observe the shift of the Raman peaks with uniaxial stress applied along the [111] direction. The average of the three peaks move as in the case of hydrostatic pressure (in a first approximation). The shift is linear up to a couple of Giga Pascals. The PDPs are known for a large amount of materials and the shift of the phonons are used to calibrate the strain.

3.3. Materials identification

With materials inspection or materials basic characterization we refer to the specific Raman spectrum of a given material. This distinction is possible in the case of crystalline or polycrystalline insulators or a few layers of materials even if they are metals. Also in some cases, in amorphous materials, there are specific bands (instead of well defined peaks) able to characterize the material, as is the case of quartz. In the case of bulk metals usually the plasmon frequency is beyond the phonon region and mask or suppress the phonon bands in the IR and the normal modes in Raman. In the figures below (Fig. 4) we can observe the different Raman spectra of two different phases of SiC [Freitas and Moore (1998)]. Another example of material basic characterization is the study of GaN quantum dots. By means of Raman scattering we are able to distinguish if the quantum dot has been grown in a polar plane of the wurtzite structure, or in a non polar plane, as is the case of Fig. 5, where the clue is also given by the PDPs. The non polar phonons are shifted only by strain, but the polar phonons are also affected by the internal electric field. The absence of quantum confined Stark effect has been also checked by PL techniques [Garro et al. (2005)].
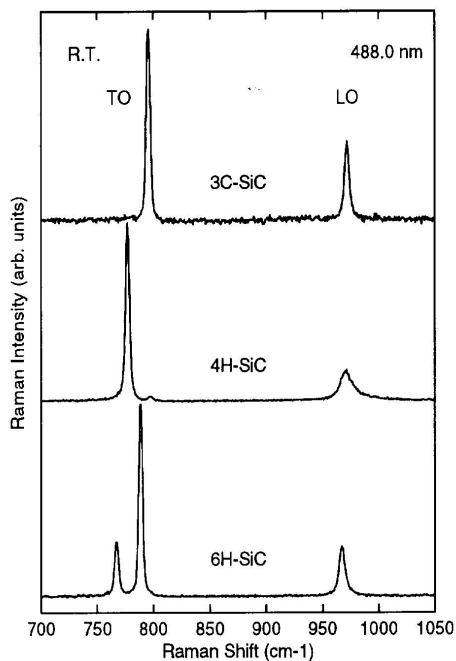
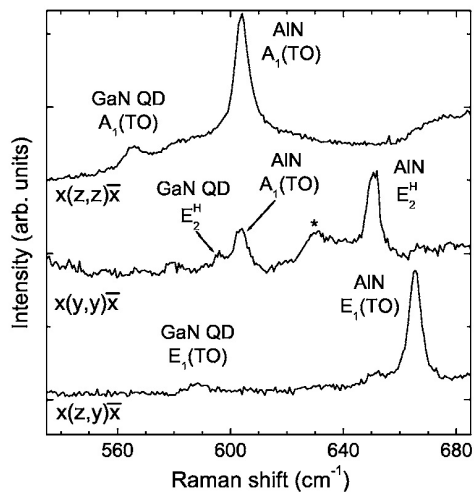Fig. 4. Distinction of different silicon carbide polytypes using Raman scattering.

Fig. 5. Different phonon modes of GaN quantum dots embedded in AlN. The non polar phonons (E_2) are only shifted due to strain, while the polar phonons (A_1 and E_1 are shifted due to the strain and electric field (quantum confined Stark effect).

3.4. Analisis of a few layers material

Nowadays, there is a tremendous scientific interest in layered materials, not only graphene, but also bismuth telluride, indium selenide, gallium selenide, molybdenum disulfide, and many other materials [Sorkin (2014)]. Raman is a suitable technique to analyze a few layers of materials and distinguish in many cases how many layers we have. This is what happens with graphene (which by the way is metallic). In Figure 6 we show the Raman spectra of HOPG and the difference between a few layers graphene [Ni el al. (2008)].
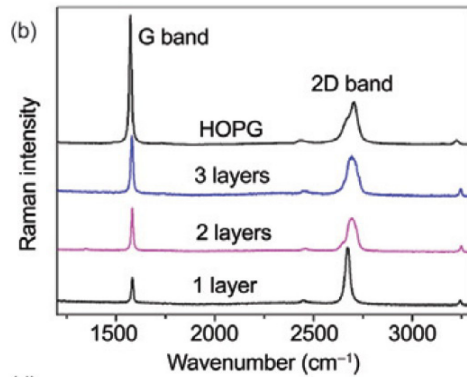
Fig. 6. Raman spectra of 1, 2, 3 graphene layers compared with that of bulk graphite (HOPG).
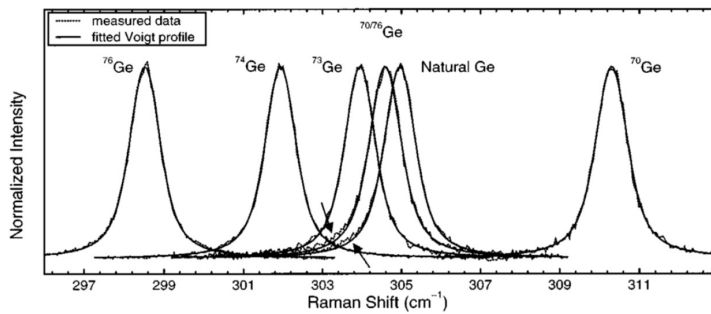

Fig. 7. Raman shift of natural Ge and enriched Ge isotopes. From the figure we can check that the shift if basically proportional to the square root of the isotopic mass.

3.5. Isotopic effects

Most of the materials supplied by the Nature or grown by means of an epitaxial technique contains the natural isotopic composition, which is different depending on the atomic element. The case of Ge is atypical because it contains a rich mixture of isotopes. Natural Ge is compose of ^{70}Ge in a 20.84%, ^{72}Ge in a 27.54%, ^{73}Ge in a 7.73%, ^{74}Ge in a 36.28% and ^{76}Ge in a 7.61%. The Raman frequency is basically proportional to the inverse of the square root of the mass. As a result, if we are able to enrich the Ge [Widulle et al. (1999)] and isolate the different isotopes, it is possible to check the mass dependence of the different isotopes. In Fig. 7 we show the shift of the Ge peaks for different isotopes

3.6. Surface optical phonons

Bulk materials have a surface, i.e. they do not go to infinity in the three directions. But in general the surface play a small role. This is not the case of a few layers of material or a quantum wire. In fact, in a quantum wire, as compared to a thin film, the specific surface can be one thousand times larger. In that case, there appear visible new phonon modes related to the surface [Cantarero (2013)], they are called surface acoustic modes. These modes appear in polar materials and they are located between the TO and the LO phonon. They are not related to quantum confinement. The modes are closer to the LO and the first SO mode can be obtained with the simple expression

$$\omega_{SO}^2 = \frac{\varepsilon_0 + \varepsilon_M}{\varepsilon_\infty + \varepsilon_M} \omega_{TO}^2 \tag{5}$$

and it is the only one observable in most of the cases. In Fig. 8 we can observe, in the case of InAs quantum wires [Möller et al. (2011)], the TO, LO and the SO close to the LO. The reason why the TO is stronger than the LO in
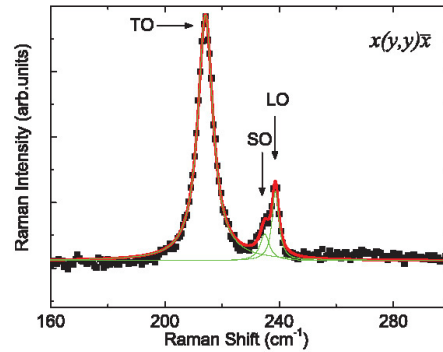
Fig. 8. Raman shift of an isolated InAs nanowire and the corresponding fit. We can clearly observe between the TO and the LO the SO mode. In the fitting can be observed much better.
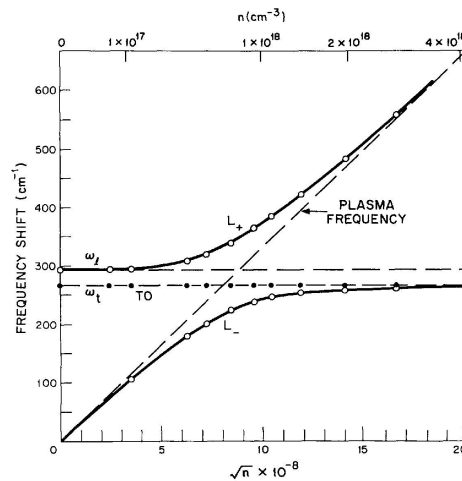

Fig. 9. Frequency shift of the GaAs phonons in a heavily doped sample due to the coupling of the LO phonon with the plasmon.

a quantum wire is evident. When the electric field has the direction of the wire, the electric boundary conditions (tangent components of the electric field must be continuous at the surface limit), while in the case of an electric field perpendicular to the wire, the boundary conditions are satisfied in a small extent. We have a contrast of permittivities at the zone boundary. Actually, the TO mode is a bulk mode [Cantarero(2013)].

The SO modes have been measured in a number of materials. See, for instance the paper of Sahoo et al.(2008) on InN nanowires. In wurtzite crystal some times it is possible to see the SO modes related to the A_1 and E_1 optical modes.

3.7. Electronic density of states

In heavily doped semiconductors, it is possible to know the electron concentration from the shift of the LO phonon. The polar mode couples with the plasmon and there is a splitting, usually called LO$^-$ and LO$^+$ or LPP$^\pm$ modes. The typical example is that of GaAs given in the book chapter of Klein(1998). In Fig. 9 we can see the splitting from electron concentrations of the order or 10^{17} to 3×10^{18} cm^{-3}. The coupling with the plasmon produces a crossing due to the mixing of states.

Actually, silicon can be doped much more than GaAs. In that case (there is no TO-LO splitting since Si is non polar) there is another way to extract the electron concentration from the Raman spectra. When the electron concentration is
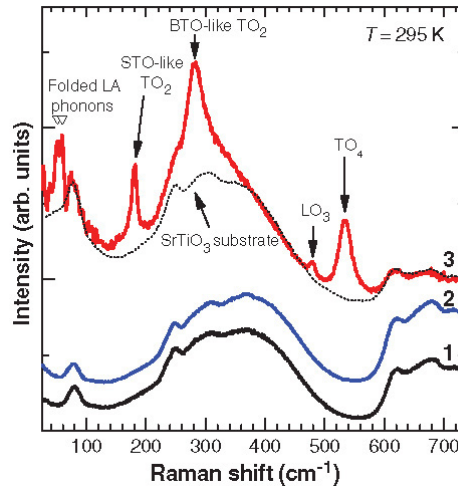
Fig. 10. Room-temperature Raman spectra of (1) a bare $SrTiO_3$ substrate (black curve); (2) a $(BTO_5/STO_4) \times 25$ superlattice (T_c = 530 K, blue curve) measured with visible excitation (514.5 nm); and (3) the same superlattice measured with 351.1 nm UV excitation (red curve). The dashed black line shows the bare $SrTiO_3$ substrate spectrum measured with 351.1 nm UV excitation. Triangles show the calculated frequencies of the first folded LA doublet.

increasing, at some point the electronic background interferes with the phonon (the transition probabilities are added before square them) and the shape of the phonon deviates from the typical Lorentzian profile (or Voigt profile), giving rise to an anisotropic lineshape known as Fano line-shape, predicted by Fano for all kind of excitation spectra. The theory of Raman scattering due to the interaction of the phonons with the electronic background was given by Belitsky et al. (1997).

3.8. Resonant Raman scattering

Although there are many other examples where Raman can be used in order to extract information on the materials in a non invasive way, one last example given here is the use of Raman scattering to measure the transition phase of STO/BTO superlattices. As it can be seen in Fig. 10, in the Raman spectra obtained with visible light only the substrate was observed [Tenne (2005)].

The use of UV light allowed to approach to the gap of the material and the signal increased several orders of magnitude, in such a way that even a 1-1 superlattice could be observed. In this experiment, the authors showed how the nanoscale can change dramatically the ferroelectric properties, in particular the Curie temperature, of BTO.

Acknowledgements

References

Anastassakis, E., Cantarero, A., Cardona, M., 1990. Piezo-Raman measurements and anharmonic parameters in silicon and diamond. Physical Review B 41, 7529-7535.
Belitsky, V. I., Cantarero, A., Cardona, M., Trallero, C., Pavlov, S. T., 1997. Feynman diagrams and Fano interference in light scattering from doped semiconductors. Journal of Physics: Condensed Matter 9, 5965-5976.
Brillouin, L., 1922. Diffusion de la lumire et des rayons X par un corps transparent homogne. Influence de ragitation thermique. Annales de Physique 17, 88-122.
Camacho, J., Cantarero, A., 2002. Vibrational properties of ZnTe at high pressures. Journal of Physics: Condensed Matter 14, 739-757.

Cantarero, A., 2012. Optical techniques for nanostructure characterization, from Encyclopedia of Nanotechnology (Vol. 3), B. Bhushan Ed., Springer.

Cantarero, A., 2013. Review of Raman scattering in semiconductor nanowires: I. Theory. Journal of Nanophotonics 7, 071598.

Cantarero, A., Trallero, C., Cardona, M., 1989. Excitons in one phonon resonant Raman scattering: Deformation potential interaction. Physical Review B 39, 8388-8397;

Comas, F., Cantarero, A., Trallero, C., Moshinsky, M., 1995. Polar optical oscillations in quantum wires and free standing wires: - The electron-phonon interaction Hamiltonian. Journal of Physics: Condensed Matter 7, 1789-1805.

Fano, U., 1961. Effects of configuration interaction on intensities and phase shifts. Physical Review 124, 1866-1878.

Freitas, Jr., J. A., Moore, W. J., 1998. Optical studies of wide bandgap carbide and nitride semiconductors. Brazilian Journal of Physics 28, 12-18.

Garro, N., Cros, A., Budagosky, J. A., Cantarero, A., Vinnatieri, A., Gurioli, M. Founta, S., Mariette, H., Daudin, B., 2009. Reduction of the internal electric field in wurtzite a-plane self-assembled quantum dots. Applied Physics Letters 87, 011101.

Hamon, C., Novikov, S., Scarabelli, L., Basabe-Desmonts, L., Liz-Marzn, L. M., 2014. Hierarchical Self-Assembly of Gold Nanoparticles into Patterned Plasmonic Nanostructures. ACS Nano 8, 10694-10703.

Klein, M. V., 1983. Electronic Raman scattering, in "Light Scattering in Solids I". Ed. M. Cardona. Springer.

Lanberg, G., Mandelstam, G. L., 1928. Eine neue Erscheinung bei der Lichtzerstreuung in Krystallen. Naturwissenschaften 16, 557-558.

Loudon, R., 1963. Theory of the first order Raman effect in crystals. Proceedings of the Royal Society A 275, 218-232.

Olguin, D., Cardona, M., Cantarero, A., 2002. Electron-phonon effects on the direct band gap in semiconductors: LCAO calculations. Solid State Communications (Review) 122, 575-589.

Möller, M., Morais de Lima, M. M., Cantarero, A., Dacal, L. C. O., Madureira, J. R., Iikawa, Chiaramonte, T., F., Cotta, M. A., 2011. Polarized and resonant Raman spectroscopy on single InAs nanowires. Physical Review B 84, 085318.

Ni, Z., Wang, Y., Yu, T., Shen, Z., 2008. Raman spectroscopy and imaging of graphene. Nano Research 1, 273-291.

Ogawa, Y., Yuasa, Y., Minami, F., Oda, S., 2011. Tip-enhanced Raman mapping of single Ge nanowires. Applied Physics Letters 99, 053112.

Raman, C. V., 1928. A new radiation. Indian Journal of Physics 2, 387-398.

Sahoo, S., Hu, M. S., Hsu, C. W., Wu, C. T., Chen, K. H., Chen, L. C., Arora, A. K., Dhara, S., 2008. Surface optical Raman modes in InN nanostructures. Applied Physics Letters 93, 233116.

Segura-Ruiz, J., Garro, N., Cantarero, A., Denker, C., Malindretos, J., Rizzi, A., 2009. Optical studies of MBE-grown InN nanocolumns: evidence of an electron accumulation layer. Physical Review B 79, 115305.

Smekal, A., 1923. Zur Quantentheorie der Dispersion. Naturwissenschaften 11, 873-875.

Sorkin, V., Pan, H., Shi, H., Quek, S. Y., Zhang, Y. W., 2014. Nanoscale transition metal dichalcogenides: structures, properties and applications. Critical Reviews in Solid State and Materials Sciences 39, 319-367.

Tenne, D. A., Bruchhausen, A., Lanzillotti-Kimura, N. D., Fainstein, A., Katiyar, R. S., Cantarero, A., Soukiassian, A., Vaithyanathan, V., Haeni, J. H., Tian, W., Schlom, D. G., Choi, K. J., Kim, D. M., Eom, C. B., Sun, H. P., Pan, X. Q., Li, Y. L., Chen, L. Q., Jia, Q. X., Nakhmanson, S. M., Rabe, K. M., Xi, X. X., 2006. Probing nanoscale ferroelectricity by ultraviolet spectroscopy. Science 313, 1614-1616.

Ulrich, C., Mroginski, M. A., Goi, A. R., Cantarero, A., Schwarz, U., Muoz, V., Syassen, K., 1996. Vibrational properties of InSe under pressure: Experiment and theory. Physica Status Solidi B 198, 121-127.

Villafuerte, M., Ferreyra, J. M., Zapata, C., Barzola-Quiquia, J., Iikawa, F., Esquinazi, P., Heluani, S. P., de Lima Jr., M. M. and Cantarero, A., 2014. Defect spectroscopy of single ZnO microwires. Journal of Applied Physics 115, 133101.

Widulle, F., Ruf, T., Gbel, A., Silier, I., Schonenherr, E., Cardona, M., Camacho, J., Cantarero, A., Kriegseis, W., Ozhogin, V. I., 1999. Raman studies of isotope effects in Si and GaAs. Physica B 263, 381-383.